ASC2024-4MPo1B-08

Effect of Zn Addition on Nb_3Sn Layer Formation in the Nb/Cu-Sn-Ti Diffusion Reaction

Koki Asai, Tsuyoshi Yagai, Taku Moronaga, Nobuya Banno.

***Abstract*—Enhancing the characteristics of Nb_3Sn superconducting wire is essential for the development of magnets for fusion reactors like ITER and DEMO. It has been established that Ti-doping has a significant effect on enhancing the upper critical magnetic field (B_{c2}). Ti is generally doped into Nb or Sn-alloys in practical Nb_3Sn superconducting wires, and it would be preferable to add Ti to the Sn side from a manufacturing perspective. However, Ti-doping on Sn sites could form some undesirable stable compounds layers at the interface with Nb as a diffusion barrier for Sn during the Nb_3Sn layer formation. It is challenging to find a new reaction route that destabilizes these compound layers in the Nb_3Sn formation process, which is expected to cause a dramatic improvement in Sn diffusion when Ti is doped to the Sn core. Nevertheless, there are few studies that fundamentally investigate this aspect. Studies have reported that Zn is effective for promoting Nb_3Sn layer formations. Therefore, in this study, specific diffusion couples of Nb/Cu/Sn were fabricated with different combinations of Ti and Zn doping to Cu and Sn and their diffusion reaction behaviors in Nb_3Sn layer formation were investigated. Besides, anticipating a potential grain refinement effect, an Mg and Zn co-doped sample was additionally fabricated. However, the grain refinement by Mg was not seen in the present wire configuration. The effect of Zn addition on promoting the Nb_3Sn layer formation appeared at 650 ℃/150 h HT, while it was not visible well at 685 ℃/100 h HT.**

***Index Terms*—Ti addition, Zn addition, Mg addition, Nb_3Sn.**

I. INTRODUCTION

Nb_3Sn superconducting wires are candidates for next-generation high-field magnets for future circular collider (FCC) projects[1], [2] and demonstration power stations (DEMO)[3]. FCC requires a non-Cu critical density of 1500 A/mm^2 at 4.2 K under a 16 T field for Nb_3Sn wires[1]. Ti is well-known for its ability to enhance the upper critical magnetic field (B_{c2}) and the critical current density (J_c) in Nb_3Sn[4],[5],[6]. Nb or Sn alloys are typically doped with Ti in Nb_3Sn superconducting wires. However, from a manufacturing perspective, Ti doping of Sn is preferable. Nevertheless, according to our previous study, in the internal tin process, the Ti doping of Sn caused undesirable NbSnTiCu quaternary phases at the diffusion interface between Nb_3Sn and Sn[7]. These phases can act as diffusion barriers for the formation of Nb from Sn. However, only a few studies have reported improvements in this aspect of Ti doping. To reduce these phases and promote Sn diffusion into Nb, in this study, a Nb/Sn/Cu composite was fabricated with Zn addition to Cu and Ti additions to the Sn core. Zn addition to Cu is thought to increase the Sn chemical potential (driving force) in Cu, which results in promoting the formation of thick Nb_3Sn layers[8], [9],[10],[11],[12].

Moreover, some studies have reported that Mg significantly affects Nb_3Sn grain refinement. Togano *et al.* reported that a small amount of Mg-doping (0.5at%) in a Cu–Sn matrix significantly affected the grain refinement[13]. Smathers fabricated Modified Jelly Roll (MJR) process wire with Sn–Mg alloy and reported that Mg-doping refined grain size and improved current carrying capacity [14]. In addition, McKinnell *et al.* also reported that Mg-doping increased J_c over 20% in the internal Sn process [15]. Yu *et al.* demonstrated that a small amount of Mg-doping (0.2wt%) to the Cu–Zn brass matrix resulted in the grain refinement of Nb_3Sn, which led to an improvement in J_c in the internal Sn process[16]. Nevertheless, the mechanism of grain refinement by Mg-doping has not yet been fully elucidated so far. In this study, the co-addition of Mg with Zn to Cu was also tested, expecting to promote Sn diffusion and simultaneously enhance Nb_3Sn grain refinement.

II. EXPERIMENTAL METHOD

We fabricated a simple diffusion couple structure of Nb/Cu/Sn to simulate the internal Sn processed wires [17],[18],[19],[20]. Zn and Mg were doped into the Cu matrix and Ti was doped into Sn and Nb (for comparison). By analyzing the layer thickness, grain size, and superconducting properties (I_c and layer J_c), the effects of adding Zn and Mg were compared with those of Ti doping during the internal tin process.

A. Samples

Four types of single diffusion coupled wires were fabricated. These four samples were named (A), (B), (C), and (D). The Cu matrix and Sn cores were inserted into the Nb-alloy tubes. The Nb/Cu/Sn alloy composite with the Cu

Submitted for review September 25, 2024
This work was supported in part by JSPS KAKENHI Grant Number JP23K04453. (Corresponding author: Nobuya Banno.)

Koki Asai is with Sophia University, Tokyo 102-8854, Japan, and with the Research Center for Energy and Environmental Materials, National Institute for Materials Science, Tsukuba, Ibaraki 305-0047, Japan (e-mail: kouki0204@eagle.sophia.ac.jp)

Tsuyoshi Yagai is with the Sophia University, Tokyo 102-8554, Japan (email: tsuyoshi-yagai@sophia.ac.jp).

Taku Moronaga is with the Research Network and Facility Services Division, National Institute for Materials Science, Tsukuba, Ibaraki 305-0047, Japan
(email: moronaga.taku@nims.go.jp)

Nobuya Banno is with the Research Center for Functional Materials, National Institute for Materials Science, Tsukuba, Ibaraki 305-0047, Japan (e-mail: banno.nobuya@nims.go.jp)

stabilizer was swaged down to 0.6 mm-diameter wires. For samples (B) and (C), Cu matrix was replaced by Cu–15wt%Zn and Cu–12wt%Zn–0.2wt%Mg. The Nb-alloy tubes were annealed at 650 ℃ for 3 h before drawing. The heat treatment (HT) was performed under vacuum at 500 ℃ for 100 h for Sn/Cu mixing and 650 ℃ for 150 h or 685 ℃ for 100 h to form the Nb_3Sn layer. Samples (A) and (D) were the same specimens used in our previous study[7].

(A)N–C–ST: Nb/Cu/Sn–1.6wt%Ti
(B)N–CZ–ST: Nb/Cu–15wt%Zn/Sn–1.6wt%Ti
(C)N–CZM–ST: Nb/Cu–12wt%Zn–0.2wt%Mg/Sn–1.6wt%Ti
(D)NT–C–S: Nb–0.8wt%Ti/Cu/Sn

B. Microstructural and microchemical analysis.

The mechanically polished cross section of each sample was observed using scanning electron microscopy (SEM) after HT. The grain size was determined by dividing a given area by the number of grains present in the fractured sample images captured using SEM in the fine-grained layer.

C. I_c measurements

The critical current I_c was measured using a standard four-probe resistive method with a magnetic field ranging from 6 to 18 T at 4.2 K. The I_c was determined by an electrical criterion of 1 μV/cm. The J_c layer was determined by dividing I_c by the area of Nb_3Sn, which was measured using image analysis.

D. S/TEM-EDS analysis

To investigate the extent of Mg diffusion into the Nb_3Sn phase, microstructural observations were performed using scanning TEM.

The sample (C) heat treated at 650 ℃ for 150 h were cut into 10-20 μm in width and 5-10 μm in thickness using a focused ion beam (Thermo Scientific Scios 2 DualBeam) from fine polished transverse cross-sections of the Nb_3Sn area. The microstructures were observed using S/TEM (JEM-ARM300F) with an acc of 300 kV) that has been installed at the Research Network and Facility Services Division of NIMS. The composition was analyzed using energy-dispersive X-ray spectroscopy (EDS).

III. Results and Discussion

A. Nb_3Sn layer formation

Fig. 1 shows the SEM images of typical cross-section of samples (A)-(D) after heat treatment at 650 ℃ for 150 h and at 685 ℃ for 100 h. The boundaries of the Nb_3Sn layer were determined from the results of EDS compositional analysis. The overall Nb_3Sn layer thicknesses for the fine-grained area are summarized in Table. I.

After heat treatment at 650 ℃ for 150 h, a stable NbSnTiCu quaternary phase layer appeared in sample (A)N-C-ST at the interface between the Nb_3Sn and Cu-Sn phase. This phase becomes a diffusion barrier for Sn to enter Nb, which leads to a thinner Nb_3Sn layer formation. Similar quaternary phases were observed in sample (B). However, these compounds were isolated and did not function as diffusion barriers for Sn.–This could account for the thicker Nb_3Sn layer observed in sample (B). In sample (C), the Mg-co-doped sample showed a slightly thinner Nb_3Sn layer than sample (B). Considering that the Mg co-addition sample exhibited a reduced effect of layer formation compared to the Zn-only addition sample, Mg seems to suppress the effect of Zn addition on the diffusion of Sn to Nb. In sample (D), NT-C-S exhibited a mixed area of coarse Nb_3Sn grains and Nb_6Sn_5 between the Nb_3Sn and Sn phases. The Sn diffusion has not progressed sufficiently at 650 ℃ heat treatment.

After heat treatment at 685 ℃ for 100 h, all the samples exhibited thick Nb_3Sn layer formation. Samples (A)–(C) developed a Nb_3Sn layer with similar thickness. The Ti compounds phase that has been present largely at 650 ℃ decreased, which indicates that the NbSnTiCu quaternary phase can be decomposed in the temperature range from 650 ℃ to 685 ℃. Sample (D) formed a significantly thicker Nb_3Sn layer. The NT sample did not form a quaternary phase during any of the heat treatment processes. Therefore, a thick Nb_3Sn layer was formed.

Table. Ⅰ Overall Nb_3Sn layer for fine grains layer thickness of sample (A)-(D).

Sample	(A)N-C-ST	(B)N-CZ-ST	(C)N-CZM-ST	(D)NT-C-S
650℃/150h	12(μm)	25(μm)	18(μm)	11(μm)
685℃/100h	23(μm)	25(μm)	27(μm)	41(μm)

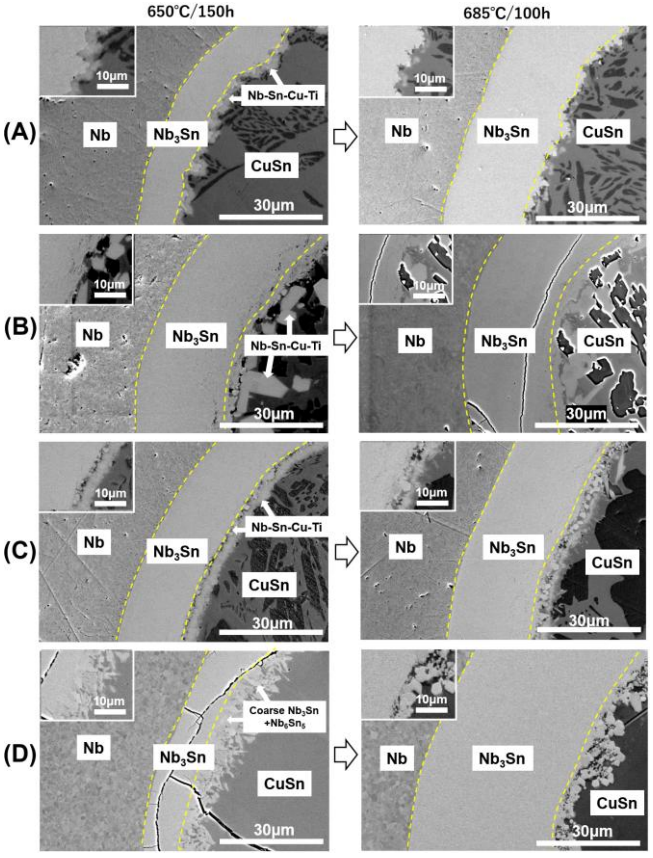

Fig. 1 Cross sectional SEM images (BSE) of the reaction layer (acceleration voltage: 20 kV) for (A) N-C-ST, (B) N-CZ-ST, (C) N-CZM-ST, (D) NT-C-S after diffusion at 650 ℃ for 150 h and at 685 ℃ for 100 h.

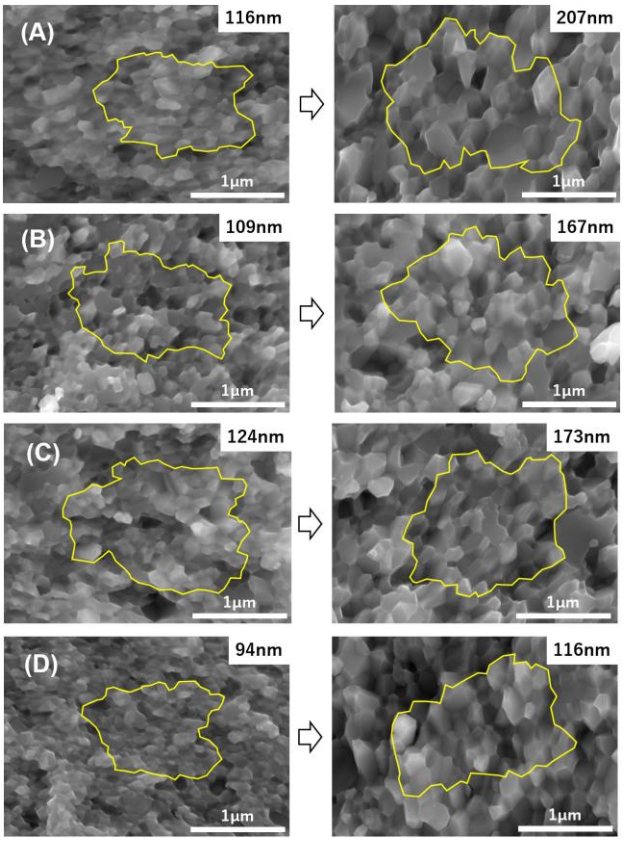

Fig .2 Fractured cross-sectional SEM images (acceleration voltage: 20 kV) in fine grain Nb_3Sn regions with the average grain size for (A) N-C-ST, (B) N-CZ-ST, (C) N-CZM-ST, (D) NT-C-S after diffusion at 650 ℃ for 150 h and at 685 ℃ for 100 h. The yellow line indicates the area used for grain size analysis.

B. Nb_3Sn grain size

Fig. 2 shows the SEM images of the fractured microstructure of the fine-grained Nb_3Sn regions of each sample, and Table II summarizes the average grain size of Nb_3Sn. Comparing samples (A) and (B), a slight grain refinement was observed in sample (B) owing to the addition of Zn in both heat treatment, that is, at 650 ℃ and at 685 ℃. In contrast, in sample (C), where Zn and Mg were co-added, a slight grain refinement was observed at 685 ℃ compared to sample (A), whereas this effect was not evident at 650 ℃. Unlike expectations, the addition of Mg did not significantly affect the grain refinement [15]. This is assumed to reflect the smaller Mg diffusion in this sample, as shown later. In sample (D), the NT specimen showed the most refined Nb_3Sn grains in both heat treatments, at 650 ℃ and at 685 ℃. It is notable that this trend differs from that of the bronze-processed Nb_3Sn wires, where the grain size is reduced when Ti is doped into the bronze matrix[21][22][23].

Table. II Average Nb_3Sn grain size of samples (A)-(D).

Sample	(A)N-C-ST	(B)N-CZ-ST	(C)N-CZM-ST	(D)NT-C-S
650℃/150h	116(nm)	109(nm)	124(nm)	94(nm)
685℃/100h	207(nm)	167(nm)	173(nm)	164(nm)

C. Superconductivity properties

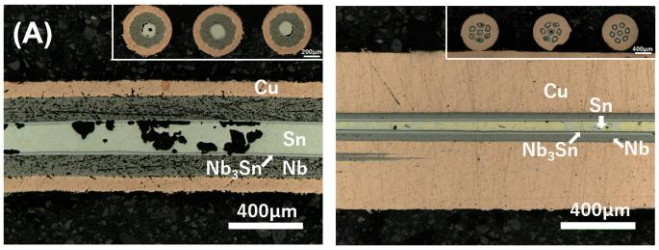

Fig. 3 longitudinal cross-sectional optional images for single core sample (left) and multifilamentary sample (right) for (A) N-C-ST after diffusion at 650 ℃ for 150 h.

Fig. 3 shows longitudinal cross-sectional optical microscope images for the single core sample and multifilamentary sample for (A)–after the heat-treatment: the multifilamentary wires were fabricated by restacking 7 single-core wires with 0.6 mm in diameter into the Cu tube with outer/inner diameter of 3/2 mm and drawing down to 0.92 mm in diameter. The cross-sectional views of the precursor wires were sound for both wires along the wire axis. However, after the heat-treatment, the missing part of the Nb_3Sn layer together with large void in the core was often found in places along the longitudinal direction in the single core wires as shown in Fig. 3(left). Reflecting this fact, the J_c properties of the single core wires were scattered from sample to sample even in the same type wires. Meanwhile, lack of Nb_3Sn was minimal in the multifilamentary wires, which results in small scattering of J_c values. Therefore, J_c properties of the multifilamentary wires are discussed below.

Fig. 4 shows the characteristics of the I_c and J_c layer for multifilamentary samples (A)–(D) as a function of the magnetic field at 4.2 K. The Zn added sample (B) exhibited higher I_c and J_c properties at 650 ℃ compared to sample (A). This is owing to the thicker Nb_3Sn layer and the smaller Nb_3Sn grain size, as shown in Fig. 1 and Table. II. However, the I_c and J_c of Zn+Mg co-doping sample (C) were decreased from the properties of sample (B). This would be consistent with the fact of the smaller Nb_3Sn layer thickness and large

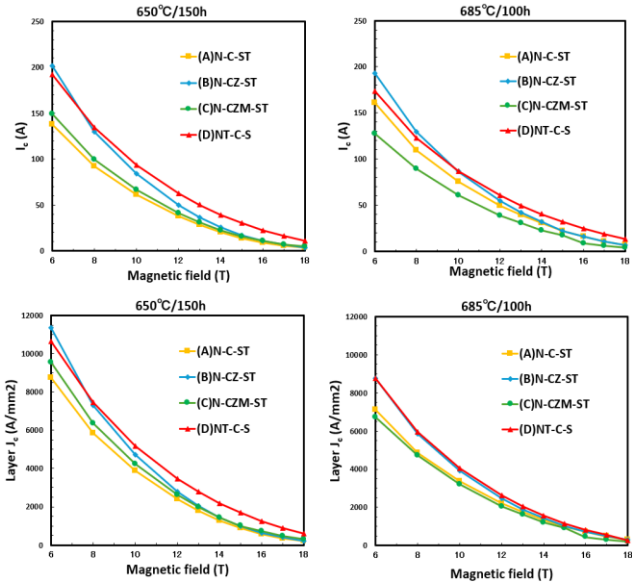

Fig .4 Characteristics of the I_c (above) and layer J_c (below) for multifilamentary samples (A)-(D) as a function of magnetic field at 4.2 K.

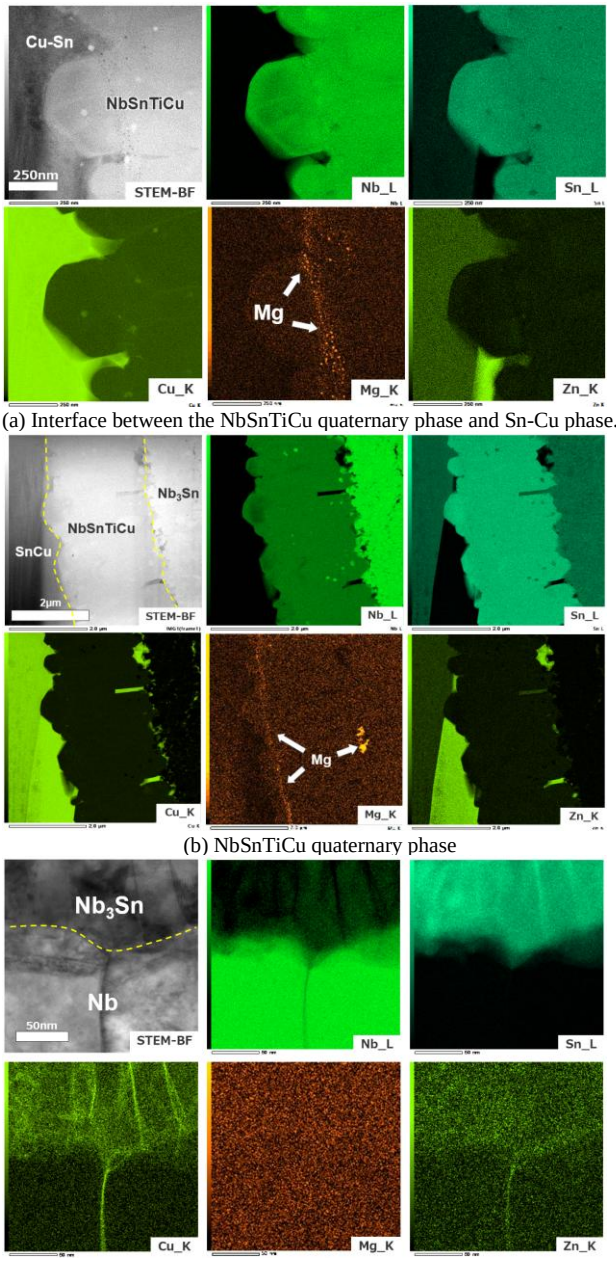

(a) Interface between the NbSnTiCu quaternary phase and Sn-Cu phase.

(b) NbSnTiCu quaternary phase

(c) Interface between Nb and Nb_3Sn

Fig. 5 STEM-BF images and EDS mapping (at%) of sample (C) N-CZM-ST heated at 650 ℃ for 150 h for (a) the interface between NbSnTiCu quaternary phase and Sn-Cu phase, (b) the NbSnTiCu quaternary phase, and (c) the interface between Nb_3Sn and Nb.

grain size. In sample (D), the NT specimen showed the highest I_c and J_c values in both heat treatments presumably reflecting the small grain size, and also thick layer thickness for 685 ℃. In all samples, it can be seen that the lower temperature heat treatment leads to higher J_c properties, which is due to the reduced grain size as shown in Table. II.

The Kramer B_{c2} estimated as the extrapolation of the Kramer plot ($J_c^{0.5}B^{0.25}$) to the horizontal axis (B: magnetic field) for samples (A)–(D) heat-treated at 650 ℃ are 20.92T, 20.42T, 21.38T and 23.61T, respectively. The Kramer B_{c2} of sample (B) was obviously small compared with (D). SEM-EDS revealed that Ti composition of the sample (B) was around 0.2at%, while that of the other samples was around 0.4at% (Nb and Sn compositions were 70-72at% and 19-21at% in all samples). The smaller B_{c2} of (B) could be attributed to the smaller Ti content. The addition of Zn promotes Sn diffusion, while on the other hand may inhibit Ti diffusion.

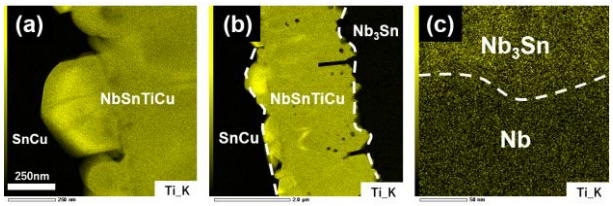

Fig. 6 EDS mapping (at%) of sample (C) N-CZM-ST heated at 650 ℃ for 150 h for (a) the interface between NbSnTiCu quaternary phase and Sn-Cu phase, (b) the NbSnTiCu phase, and (c) the interface between Nb_3Sn and Nb.

D. S/TEM-EDS analysis for Zn+Mg co-doped sample

Fig. 5 shows the STEM-BF images and EDS mapping (at%) of sample (C) N-CZM-ST heated at 650 ℃ for 150 h: (a) the interface between NbSnTiCu quaternary phase and Sn–Cu phase, (b) the interface between NbSnTiCu quaternary phase and Nb_3Sn, and (c) the interface between Nb_3Sn and Nb. Ti mappings of sample (C) N-CZM-ST heated at 650 ℃ for 150 h for (a) the interface between NbSnTiCu quaternary phase and Sn-Cu phase, (b) the NbSnTiCu phase, and (c) the interface between Nb_3Sn and Nb are exhibited in Fig. 6. Ti can be detected strongly in NbSnTiCu phase and weakly in Nb_3Sn.

The contrast of Mg (orange) has been slightly increased for better visibility. Mg were observed in the NbSnTiCu phase, but little in the Nb_3Sn phase. In the EDS spectrum for the area shown in Fig. 5(c), Mg peaks were not detected. We could say that Mg did not almost diffuse into Nb_3Sn at the reaction front.

In the previous internal-tin wires with Mg addition, Ti was doped into Nb[14],[15],[24]. In contrast, in this work, Ti was doped into Sn, which resulted in the formation of NbSnTiCu phase. Mg seems to have been almost trapped in this phase and stabilize this phase. This would be the reason why no grain refinement effect was seen.

IV. CONCLUSION

This study compared the effects of the addition of Zn and Zn–Mg to Cu on Ti-added samples. First, we found that Zn isolates NbSnTiCu phase at the interface of Nb_3Sn and Cu–Sn, which results in promoting the Nb_3Sn phase formation. However, contrary to expectations, the NbSnTiCu phase could not be reduced by Zn addition. Grain refinement was found in Zn-addition. Mg was trapped in the NbSnTiCu phase in the case of Ti doping to Sn core and did not almost diffuse into Nb_3Sn: no grain refinement effect by Mg doping was seen. If Mg can diffuse into Nb_3Sn phase, the Zener pinning effect might be also expected for the grain refinement. However, whether Mg diffuses into Nb_3Sn or not has not been clarified. This seems to be still an open question. The addition of Ti to the Nb sample (NT) yielded favorable results in terms of layer thickness and grain size. Combining the NT sample with Zn, higher Mg contents, and optimized heat treatments may be more effective in improving these properties.

REFERENCES

[1] A. Ballarino and L. Bottura, "Targets for RandD on Nb3Sn conductor for high energy physics," *IEEE Transactions on Applied Superconductivity*, vol. 25, no. 3, Jun. 2015, doi: 10.1109/TASC.2015.2390149.

[2] D. Schoerling *et al.*, "The 16 T Dipole Development Program for FCC and HE-LHC," *IEEE Transactions on Applied Superconductivity*, vol. 29, no. 5, Aug. 2019, doi: 10.1109/TASC.2019.2900556.

[3] N. Mitchell *et al.*, "Superconductors for fusion: A roadmap," Oct. 01, 2021, *IOP Publishing Ltd*. doi: 10.1088/1361-6668/ac0992.

[4] K. Tachikawa, T. Asano, and T. Takeuchi, "High-field superconducting properties of the composite-processed Nb 3Sn with Nb-Ti alloy cores," *Appl Phys Lett*, vol. 39, no. 9, pp. 766–768, 1981, doi: 10.1063/1.92847.

[5] T. Asano, Y. Iijima, K. Itoh, and K. Tachikawa, "Effects of Titanium Addition to the Niobium Core on the Composite-Processed Nb3Sn*," 1986. doi: 10.2320/matertrans1960.27.204.

[6] T. Takeuchi, T. Asano, Y. Iijima, and K. Tachikawa, "Effects of the IVa element addition on the composite-processed superconducting Nb3Sn," *Cryogenics (Guildf)*, vol. 21, no. 10, pp. 585–590, Oct. 1981, doi: 10.1016/0011-2275(81)90226-5.

[7] T. Morita, T. Yagai, and N. Banno, "Impact of Ti-doping position on Nb3Sn layer formation in internal Sn-processed Nb3Sn superconducting wires," *Cryogenics (Guildf)*, vol. 122, Mar. 2022, doi: 10.1016/j.cryogenics.2022.103420.

[8] N. Banno, Y. Miyamoto, and K. Tachikawa, "Multifilamentary Nb3Sn Wires Fabricated Through Internal Diffusion Process Using Brass Matrix," *IEEE Transactions on Applied Superconductivity*, vol. 26, no. 3, Apr. 2016, doi: 10.1109/TASC.2016.2531123.

[9] K. Tachikawa, N. Banno, and Y. Miyamoto, "Studies on New Internal Tin Processed Nb3Sn Wires with Brass Matrix," 2016, *Japan Institute of Metals (JIM)*. doi: 10.2320/jinstmet.JC201613.

[10] H. Wada, M. Kimura, and K. Tachikawa, "Superconducting properties of the composite-processed Nb3Sn superconductor with the Cu-Sn-Zn matrix," *J Mater Sci*, vol. 13, no. 9, pp. 1943–1950, Sep. 1978, doi: 10.1007/BF00552901.

[11] N. Banno, T. Morita, T. Yagai, S. Kawashima, and Y. Murakami, "Fundamental Study on the Effect of Zn Addition into Cu Matrix in DT Method Nb3Sn Conductors," *IEEE Transactions on Applied Superconductivity*, vol. 30, no. 4, Jun. 2020, doi: 10.1109/TASC.2020.2972209.

[12] N. Banno, "Low-temperature superconductors: Nb_3Sn, Nb_3Al, and NbTi," *Superconductivity*, vol. 6, p. 100047, Jun. 2023, doi: 10.1016/j.supcon.2023.100047.

[13] K. Togano, T. Asano, and K. Tachikawa, "Effects of magnesium addition to the CuSn matrix in the composite-processed Nb_3Sn superconductor," *Journal of The Less-Common Metals*, vol. 68, no. 1, pp. 15–22, 1979, doi: 10.1016/0022-5088(79)90268-6.

[14] David B. Smathers., "PROCESS FOR MAKING FLAMENTARY SUPERCONDUCTORS USING TN-MAGNESUM EUTECTCS," *United States Patent*, Nov. 1990.

[15] J. C. Mckinnell, M. B. Siddall, P. M. O'larey, D. B. Smathers, T. Wah, and C.-A. P. O. Box, "INCREASED SUPERCONDUCTING CRITICAL CURRENT DENSITY IN INTERNAL TIN NIOBIUM-TIN (Nb3Sn) COMPOSITE WIRES BY MAGNESIUM DOPING," *Teledyne Wah Chang-Albany*, 1994.

[16] Z. Yu, N. Banno, Y. Zhao, and K. Tachikawa, "The effects of Mg doping on the microstructure and transport properties of internal tin-processed brass matrix Nb 3 Sn superconductors," *Supercond Sci Technol*, vol. 32, no. 3, Jan. 2019, doi: 10.1088/1361-6668/aaf61a.

[17] M. B. Field, Y. Zhang, H. Miao, M. Gerace, and J. A. Parrell, "Optimizing Nb3Sn conductors for high field applications," *IEEE Transactions on Applied Superconductivity*, vol. 24, no. 3, 2014, doi: 10.1109/TASC.2013.2285314.

[18] J. A. Parrell, Y. Zhang, M. B. Field, P. Cisek, and S. Hong, "High field Nb3 Sn conductor development at Oxford superconducting technology," in *IEEE Transactions on Applied Superconductivity*, Jun. 2003, pp. 3470–3473. doi: 10.1109/TASC.2003.812360.

[19] J. A. Parrell *et al.*, "Internal tin Nb_3Sn conductors engineered for fusion and particle accelerator applications," *IEEE Transactions on Applied Superconductivity*, vol. 19, no. 3, pp. 2573–2579, Jun. 2009, doi: 10.1109/TASC.2009.2018074.

[20] X. Xu, E. Collings, M. Sumption, C. Kovacs, and X. Peng, "The effects of Ti addition and high Cu/Sn ratio on Tube Type $(Nb, Ta)_3Sn$ strands, and a new type of strand designed to reduce unreacted Nb ratio," *IEEE Transactions on Applied Superconductivity*, vol. 24, no. 3, pp. 12–15, 2014, doi: 10.1109/TASC.2013.2291159.

[21] E. N. Popova, I. L. Deryagina, and E. G. Valova-Zaharevskaya, "The Nb_3Sn layers formation at diffusion annealing of Ti-doped multifilamentary Nb/Cu-Sn composites," *Cryogenics (Guildf)*, vol. 63, pp. 63–68, 2014, doi: 10.1016/j.cryogenics.2014.07.007.

[22] I. L. Deryagina, E. N. Popova, E. I. Patrakov, and E. G. Valova-Zaharevskaya, "Effect of Nb_3Sn layer structure and morphology on critical current density of multifilamentary superconductors," *J Magn Magn Mater*, vol. 440, no. August 2016, pp. 119–122, 2017, doi: 10.1016/j.jmmm.2016.12.091.

[23] S. Santra *et al.*, "Insight into the effect of Ti-addition on diffusion-controlled growth and texture of Nb_3Sn intermetallic superconductor phase," *Materialia (Oxf)*, vol. 6, no. January, p. 100276, 2019, doi: 10.1016/j.mtla.2019.100276.

[24] B. A. Glowaccki, “Influence of the Tin Diffusion Process in ul t i fil ame n t as y-Cu-Sn-Mg-Ta Wire on Nb3Sn Inter-Filamentary,” 1997.